Risks of Occupational Vibration Exposures

VIBRISKS

FP5 Project No. QLK4-2002-02650
January 2003 to December 2006

Annex 10 to Final Technical Report

Title: Biodynamic modelling of the finger

Author: Gérard Fleury

Organisation: Institut National de Recherche et de Sécurité, France

European Commission

Quality of Life and Management of Living Resources Programme
Key Action 4 - Environment and Health

5th February 2007

Biodynamic Modelling of the Finger

1. Objective

According to Task 3.3 named “Biodynamic modelling of hand-arm system”, the work content has changed from the original description. In the first proposal, it had been proposed to develop a model of the upper limb (including the hand, the arm and the shoulder) and to solve the inverse problem formulated as : calculate the internal forces (exerted by the muscles) knowing the external forces (gripping, pushing, loads…). Because the flexibility of the human tissues is not taken into account, this type of model is of interest to assess the impedance of the upper limb at frequencies below about 50 Hz. However neurological and vascular effects which constitute the main target of this contract are mainly observed at higher frequencies. So, any correlation nor comparison could be expected between experimental work of WP3 and the model output.

Therefore it has been decided to focus on the modelling of the dynamic behaviour of soft tissues: the idea is now to develop a model able to predict how vibration propagate in the human tissues and to calculate internal mechanical properties such as pressure-field or strain, whose measurement is technically impossible to perform. The main interest of such a model will be to correlate the physiological response to vibration (output from WP3.1 and WP3.2) with local high levels of pressure or strain. In that way, it is expected to bring keys to the understanding of the vascular and neurological effect of vibration.

A model was elaborated to predict the mechanical response for a pre-stressed finger submitted to vibration.

2. Method

The Finite Element Method (FEM) was chosen to achieve calculations of local internal quantities such as stresses or strains inside the finger. It was assumed that these quantities are correlated with physiological troubles due to vibration exposure; they are difficult to obtain by measurements, thus their prediction by means of numerical simulations becomes of interest to have a better understanding of physiological troubles due to vibration exposure.

A first model of a forefinger cross section was developed. This model is limited to two-dimensional analysis. Thus, INRS worked at the extension of this model towards a 3D model for the forefinger. Real finger geometries were digitised and discretized in meshes to perform FEM calculations. INRS used a commercial FEM software to perform the simulations with the 3D model but difficulties were encountered to make the model stable. Consequently INRS performed some calculations with the open source software Code Aster for FEM analysis to investigate its capabilities. This software, released under the General Public Licence, showed some interested capabilities and offered possibilities to develop adapted numerical routines to achieve our objective. But these developments were not planned in the project and would require too much time and costs. Finally efforts were devoted to the response study of a forefinger 3D local model with simplified geometry. Only soft tissues between the vibrating rigid plate and the bone were considered and modelled as a parallelepipedic volume with viscohyperelastic behaviour.

3. Results

3.1 Two-dimensional Model

J. Wu in [1] has developed a finite element model in order to investigate theoretically the effects of static compression on the vibration modes of a fingertip. An in-plane finite element model of the fingertip tissue was formulated on the basis of the anatomical structure and the non linear elastic material properties of the soft tissue. The vibration modes of a fingertip model were analysed under different deformation states. Results show that the modal vibration characteristics of the fingertip increase with the preload. All calculations were performed with the commercial Finite Element software Abaqus. The first task to achieve for INRS was to look at the feasibility of these calculations by using Samcef, which is the Finite Element Program available at INRS. Thus an in-plane model of an elliptical cross-section at the fingertip was build. The fingertip was assumed to be symmetric around the bone. Thus, only half of a fingertip was modelled, as shown in figure 1.

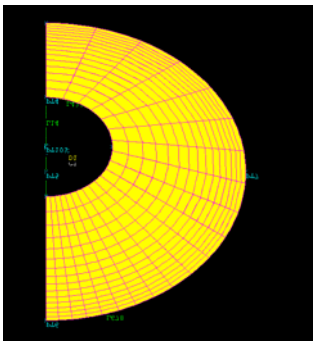

Figure 1: Mesh for an half cross-section at the fingertip

The model is composed of a rigid bone surrounded with viscohyperelastic soft tissues. The surface of the soft tissue is assumed to be in contact with a rigid plate, representing the vibrating machine. The rigid plate is subjected to a prescribed vertical displacement to realise a pre-constraint in the soft tissue occurring during gripping the machine or its handle. A modal analysis of the pre-stressed soft tissues is performed for several level of compression and the mode shapes were computed (figure 2). All the calculations were compared to the results obtained by J. Z. WU [1] [2] and identical conclusions could be drawn. Effects of the static deformation state on the vibration modes were observed.

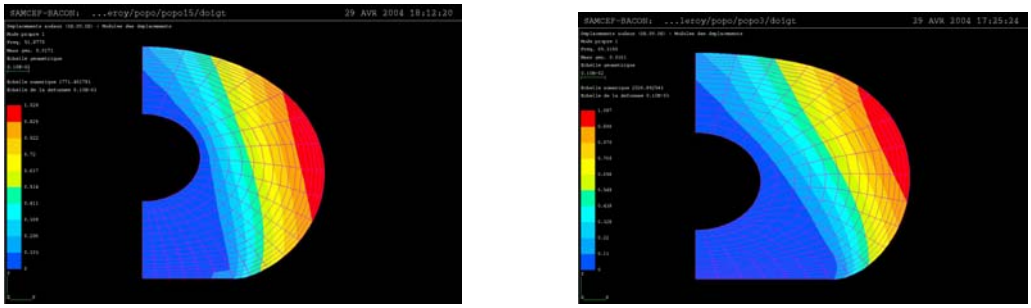

1.5 mm deflection , f = 52 Hz 3 mm deflection, f = 65 Hz

Figure 2 : 1st mode shape for two different deflections.

3.2 Towards a 3-dimensional Model

The dynamical response of a pre-compressed forefinger was modelled by an in-plane model representing a cross-section of a forefinger. This simple model was a first step to model the local behaviour of the pre-compressed forefinger, at the fingertip for example. To extend the model prediction to the behaviour of the whole-finger, the same 2D-model may be used with the assumption that the forefinger cross-section does not vary along the finger axis. This assumption is obviously wrong and the 2D model may produce results far from experimental measurements. Therefore a three-dimensional model has been worked out taking into account a real 3D geometry. This part of the work was carried out during a 6 month student engineer's trainee to obtain the degree of master in mechanical modelling and simulation from University Claude Bernard in Lyon [6]. The 3D model comprised the three finger phalanxes surrounded by soft tissues. Geometry files of the three phalanx have been downloaded from the website [3]. The outer surface of a forefinger, i.e. the skin, was digitised and numerically processed in order to include the phalanx geometry in the digitised outer finger surface. A 3D geometry model was thus obtained and prepared to be meshed.

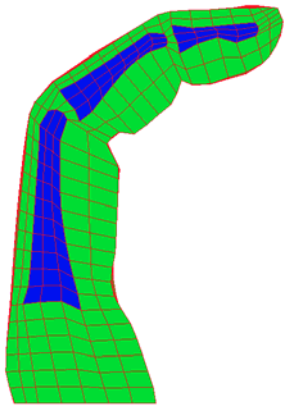

Figure 3: Longitudinal section of the three-dimensional forefinger mesh

The mesh was automatically generated using hexahedra elements with the elements size parameterised. The figure 3 shows a longitudinal section of the forefinger mesh. Blue parts corresponds to the three phalanx sections and green elements models the soft tissues volume. Visco-hyperelastic constitutive equations used in [1,2] are used to model the behaviour of the soft tissues. Bone behaviour is supposed to remain rigid. Therefore nodes on bone outer surface are interconnected with rigid connections. Loading conditions like displacement functions are applied on these nodes in order to simulate a finger motion. A rigid steel plate or a cylinder is added to take into account of the machine handle. Soft tissues deformations simulations were then performed but no solution was obtained due to many numerical problems. Some simulation tests were performed with another Finite Element Program, which is available in the frame of a General Public licence [4], but first results could not be achieved for all loading cases due to numerical instabilities. Secondly results which were obtained, were not obtained with a sufficient trust level to be published. Several reasons are likely to explain why the calculations did not converge, the main reason being probably the use of sophisticated constitutive equations to model time-dependant (visco) non-linear (hyper) elastic behaviour of soft tissues.

3.3 Analysis of a simplified 3-dimensional Model

In a third step, a simplified 3D model was developed and investigations were focused on the constitutive equations used to describe the viscohyperelastic deformation behaviour of soft tissues. Only soft tissues between the vibrating rigid plate and the distal phalanx were considered and modelled as a parallelepipedic volume viscohyperelastic behaviour (see Figure 4).

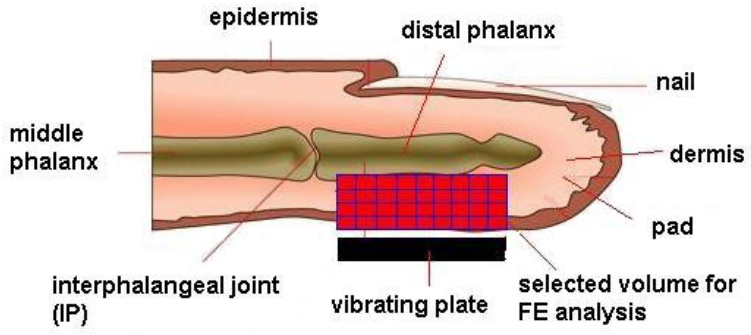

Fig. 4: Longitudinal finger section. The area used for FE analysis is the red grid volume (10 x 10 x 4 mm).

3.3.1. The time-independent non-linear elastic deformation (hyperelastic)

Models used to describe hyperelastic behaviour are based on the definition of an hyperelastic potential W. The Samcef code offers several possibilities such as Money-Rivlin, Hart-Smith, Ogden or Hyperfoam to simulate hyperelastic behaviour. The Hyperfoam definition is commonly used to model finite deformation for structure made with plastic foam like seat cushion. This potential was also chosen in [1,2] to model the behaviour of soft tissues in a finger. The potential W is expressed as function of principal stretch ratios λ_i and material parameters μ_i, α_i and β_i.

$$W = \sum_{i=1}^{N} \frac{2\mu_i}{\alpha_i^2}\left[\lambda_1^{\alpha_i} + \lambda_2^{\alpha_i} + \lambda_3^{\alpha_i} - 3 + \frac{1}{\beta_i}\left(J^{-\alpha_i\beta_i} - 1\right)\right] \qquad \text{eq. 1}$$

Based on this definition, the force required to extend or compress a parallelepipedic volume in one direction is given as a function of the brick length in the force direction. This force is expressed as:

$$F = S_0 \frac{2l_0}{l} \sum_{i=1}^{N} \frac{\mu_i}{\alpha_i}\left(\left(\frac{l}{l_0}\right)^{\alpha_i} - \left(\frac{l}{l_0}\right)^{-\upsilon\alpha_i}\right) \qquad \text{eq. 2}$$

where :

F : applied force
l: length of the deformed brick
l_0: initial length of the brick
S_0: Cross-section of the brick
υ, α_i, μ_i: material parameters

This equation is valid for compression and tensile loading. First, the displacement/force relation was checked to the relation obtained by a finite element calculations performed with Samcef with material parameters given in [1,2]. Both calculations led to the same results. In a second step, the relation (eq. 2) was used to investigate sensitivity of material parameters on the displacement-force relation. This study shows that modifying of +/-2% the value of some material parameters given in [1,2] led to large modification of the displacement-force relation. For some cases, a light modification of material parameter led to abnormal displacement-force relation such as a positive force for a compressed state.

The compressibility behaviour was investigated by comparing previous results with forces resulting from an uniaxial stressed material cube confined in a rigid container, i.e. the transversal displacement at the lateral faces are fixed. Figure 5 shows the comparison between confined and unconfined state and large differences are obtained during compression test.

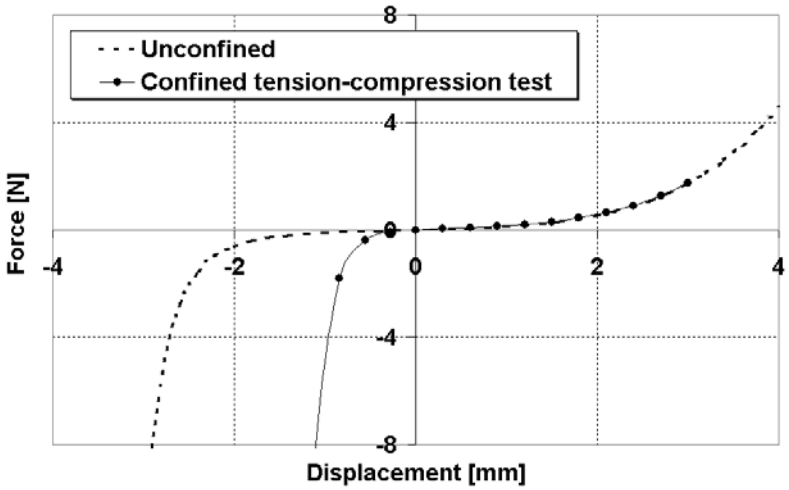

Figure 5: Comparison of the displacement-force relation during a tension-compression test applied on a confined and unconfined cube.

The shear force required to deform a cube was also expressed as a function of the lateral displacement, material and geometry parameters. Analytical results are in agreement with those obtained by Finite Element calculations and no singularity was found with this material parameter set.

3.3.2. The time-dependent non-linear elastic deformation (viscohyperelastic)

According to [5], the stress is computed at a given time t by:

$$\sigma = \frac{\partial W(t)}{\partial E} + \int_0^t \dot{g}(\tau') \frac{\partial W(t-\tau')}{\partial E} d\tau' \qquad \text{eq. 3}$$

where σ is the Kirchhoff-Treffz stress, E the Green strain and W is the previous defined potential. This equation is an hereditary integral formulation. A serial function was selected for g. The so-called Prony series were used:

$$g(t) = 1 - \sum_k \omega_k \left(1 - e^{-\frac{t}{\tau_k}}\right) \qquad \text{eq. 4}$$

where:

ω_k and τ_k are weighting coefficients and characteristic times.

The deformations are defined as follows:

$\lambda=1+\varepsilon$ $\qquad E=\varepsilon+0.5*\varepsilon^2$ $\qquad \lambda^2=1+2E$ eq. 5

where:

λ: stretch ratios

E: Green deformation

ε: nominal strain

Based on equations 3. and 4., the force F required to compress a parallelepipedic volume with a constant compression rate in one direction was expressed as a time function [8].

$$F(t)=S_0\lambda\left\{2\sum_{i=1}^{N}\frac{\mu_i}{\alpha_i}\left(\lambda^{\alpha_i-2}-\lambda^{-\upsilon\alpha_i-2}\right)-\frac{1}{\dot{\varepsilon}_0}\sum_k\frac{\varpi_k}{\tau_k}e^{-\frac{\lambda}{\dot{\varepsilon}_0\tau_k}}\left(\int_1^{\lambda}e^{\frac{u}{\dot{\varepsilon}_0\tau_k}}2\sum_i\frac{\mu_i}{\alpha_i}\left(u^{\alpha_i-2}-u^{-\upsilon\alpha_i-2}\right)du\right)\right\} \quad \text{eq.6}$$

where:

$l(t)=l_0-v_0t$

v_0 : displacement velocity

$\lambda(t)=1+\dot{\varepsilon}_0\,t$

$\dot{\varepsilon}_0=-\frac{v_0}{l_0}$: compression rate

First, the displacement/force expression 6 was checked by comparing with the force obtained by a finite element calculation performed on the finger model with a cross section of (10 x 10) mm² and a length of 4 mm in the force direction with material parameters given in [1,2]. Calculations were conducted up to 3 mm compression reached in 10 seconds. Both calculations led to the same results. Using the expression 6, the maximal force obtained at 3 mm compression was calculated for several compression time. Figure 6 shows that the maximal force decreases with increasing compression time and illustrates the relaxation phenomenon.

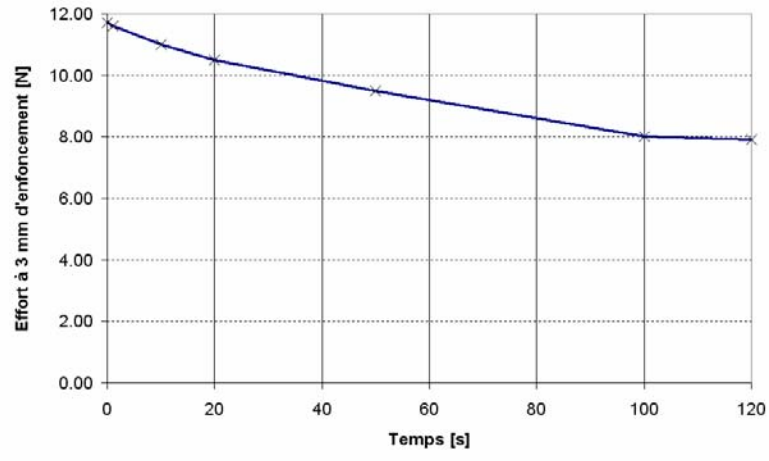

Figure 6. Influence of compression time on the force at 3 mm compression on a brick (cross section: (10 x 10) mm²; initial length in the force direction: 4 mm)

In a second step, the temporal evolution of the force was computed during a two-step test, with an initial compression test at constant deformation rate from time 0 to time t_0 and a consecutive step at constant strain i.e. a relaxation test. The force during the relaxation test was computed as:

$$F(t) = S_0 \lambda_0 \left\{ \begin{array}{l} \displaystyle\sum_i \frac{2\mu_i}{\alpha_i} \left({\lambda_0}^{\alpha_i - 2} - {\lambda_0}^{-\nu\alpha_i - 2} \right) \left(1 - \sum_k \varpi_k \left(1 - e^{-\frac{(t-t_0)}{\tau_k}} \right) \right) \\ \displaystyle -\frac{1}{\dot{\varepsilon}_0} \sum_k \frac{\varpi_k}{\tau_k} e^{-\frac{\lambda_0}{\dot{\varepsilon}_0 \tau_k}} \left(\int_1^{\lambda_0} e^{\frac{u}{\dot{\varepsilon}_0 \tau_k}} \sum_i \frac{2\mu_i}{\alpha_i} \left(u^{\alpha_i - 2} - u^{-\nu\alpha_i - 2} \right) du \right) e^{-\frac{(t-t_0)}{\tau_k}} \end{array} \right\} \qquad \text{eq. 7}$$

where:

t_0: Duration of the compression test at constant strain rate

λ_0: stretch ratio at time t_0

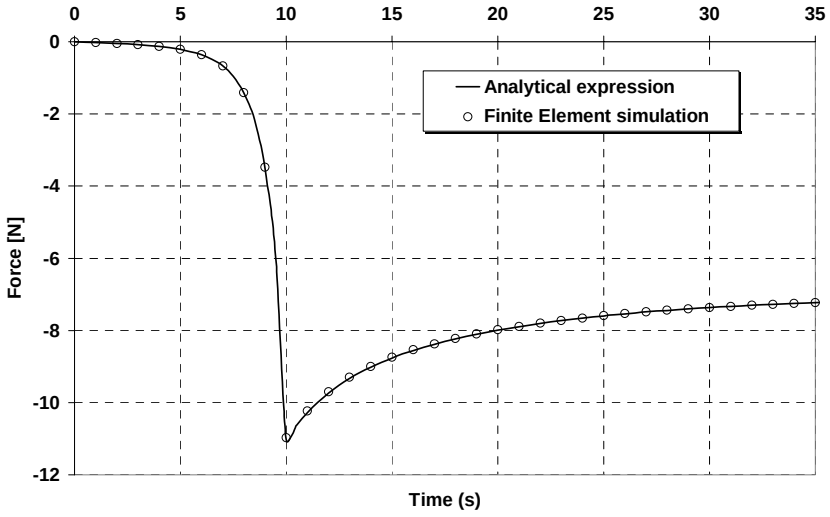

Figure 7. Temporal evolution of the applied force; from 0 to 10 seconds, the brick is compressed from 0 to 3 mm compression; from 10 to 35 seconds, the compression is maintained at 3 mm; brick of cross section: (10 x 10) mm² and initial length in the force direction: 4 mm.

According to figure 7, the expression 7 and finite element calculations give identical results. This is here to notice that the finite element program shows some numerical instabilities to calculate the force for at a time higher than 35 seconds. This is not due to the behaviour's law itself but to the fact that the steady state is reached. According to figure 7, the steady state is reached after about 20 second relaxation. The maximal force decreases from –11 Newtons to –7 Newtons. Viscosity effects on obtained forces are therefore significant.

In a third step, the time history of the force was expressed for the following displacement loadcases including compression, relaxation and consecutive sinusoidal excitation. Time-dependent effects of the non-linear elastic deformation (viscohyperelastic) were taken into account. Following displacement loadcases were applied (see figure 8):

- compression from l_0=4 mm to l_1=1 mm during t_0=10 seconds.
- relaxation from t_0=10 seconds to t_1=20 seconds, i.e. the deformation was kept remained constant.

- consecutive sinus excitation at a frequency of 1. Hz with a displacement magnitude of 0.01 mm.

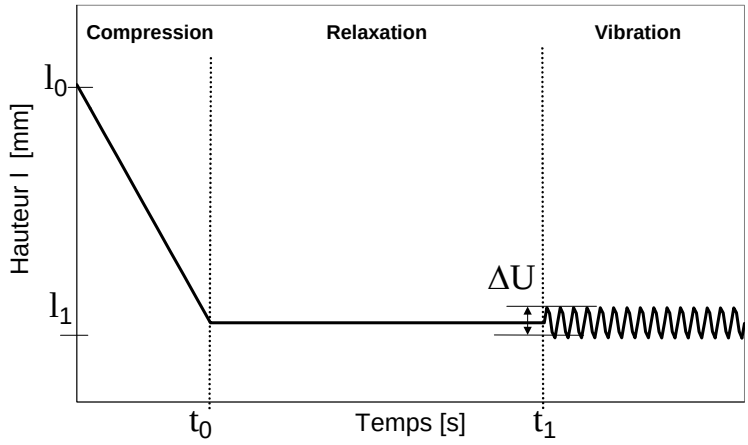

Figure 8 : Displacement applied at the upper surface of the model, compression – relaxation – sinusoidal excitation

The force during the vibration excitation was computed as:

$$F(t)=S_0\left(\lambda_0+\frac{\Delta U}{2}\sin\left(\omega\left(t-t_1\right)\right)\right)\left\{\begin{array}{l}2\sum_1^N\frac{\mu_i}{\alpha_i}\lambda_0^{\alpha_i-2}-\lambda_0^{-\nu\alpha_i-2}\left(1-\sum_k\varpi_k\left(1-e^{-\frac{t-t_0}{\tau_k}}\right)\right)\ldots\\ -\frac{2}{\dot{\varepsilon}_0}\sum_k\sum_i\frac{\mu_i}{\alpha_i}\frac{\varpi_k e^{-\frac{1}{\dot{\varepsilon}_0\tau_k}}e^{-\frac{t}{\tau_k}}}{\tau_k}\left(\int_1^{\frac{l_1}{l_0}}e^{\frac{u}{\dot{\varepsilon}_0\tau_k}}\left(u^{\alpha_i-2}-u^{-\nu\alpha_i-2}\right)du\right)\ldots\\ +\Delta U\sum_i\frac{\mu_i}{\alpha_i}\left(\left(\alpha_i-2\right)\lambda_0^{\alpha_i-2}-\left(-\nu\alpha_i-2\right)\lambda_0^{-\nu\alpha_i-2}\right)\\ \left[\lambda_0\sin\left(\omega\left(t-t_1\right)\right)-\sum_k\frac{\varpi_k}{1+\tau_k^{\,2}\omega^2}\left(\left(\sin\left(\omega\left(t-t_1\right)\right)-\omega\tau_k\cos\left(\omega\left(t-t_1\right)\right)\right)+\omega\tau_k e^{-\frac{t-t_1}{\tau_k}}\right)\right]\end{array}\right\}$$

eq. 8

where:

μ_i, α_i, ν: material parameters to describe hyperelastic behavior of soft tissues
ω_k, τ_k: are material parameters to describe viscous behavior of soft tissues
S_0: cross section of the model
l_0: initial length of the model
$\dot{\varepsilon}_0$: deformation rate during compression
λ_0: elongation during relaxation
ΔU: displacement magnitude of the sinusoidal excitation
ω: frequency of the sinusoidal excitation
t_0: time when compression stops and relaxation begins
t_1: time when relaxation stops and vibration begins

The figure 9 shows the response force calculated by the finite element software compared to its analytical expression given by eq. 8.

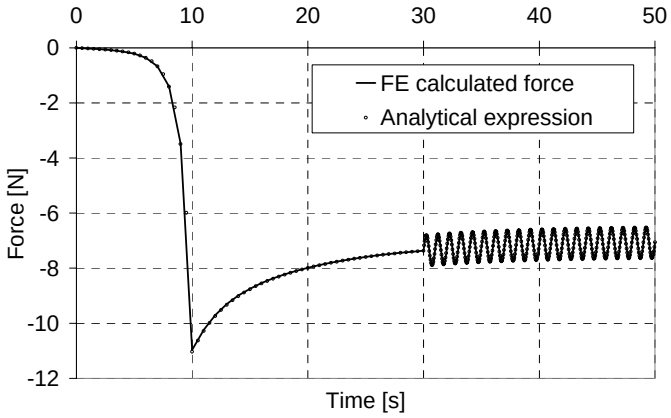

Figure 9. Time-history of the force. Finite Element calculations and analytical expression

3.3.3. Expression of the impedance

The driving point impedance of the pre-compressed volume was expressed [8] as a function of the frequency by:

$$Z = \left|\frac{F}{V}\right| = \frac{2S_0}{l_0}\left(\sum_i \frac{\mu_i}{\alpha_i}\left((\alpha_i - 2)\lambda_0^{\alpha_i - 2} - (-\nu\alpha_i - 2)\lambda_0^{-\nu\alpha_i - 2}\right)\right)$$
$$\sqrt{\left(\sum_k \frac{\varpi_k \tau_k}{1+\tau_k^2\omega^2}\right)^2 + \frac{1}{w^2}\left(\frac{\sum_1^N \frac{\mu_i}{\alpha_i}\lambda_0^{\alpha_i-2} - \lambda_0^{-\nu\alpha_i-2}}{\sum_i \frac{\mu_i}{\alpha_i}\left((\alpha_i-2)\lambda_0^{\alpha_i-2} - (-\nu\alpha_i-2)\lambda_0^{-\nu\alpha_i-2}\right)}\left(1-\sum_k \varpi_k\right) + 1 - \sum_k \frac{\varpi_k}{1+\tau_k^2\omega^2}\right)^2}$$

eq. 9

The impedance given by eq.9 was validated by comparison between its results to that given by the equivalent finite element calculation. Both led to identical results. The impedance calculated by eq. 9 is also the impedance of the rheological model shown in figure 10 [8].

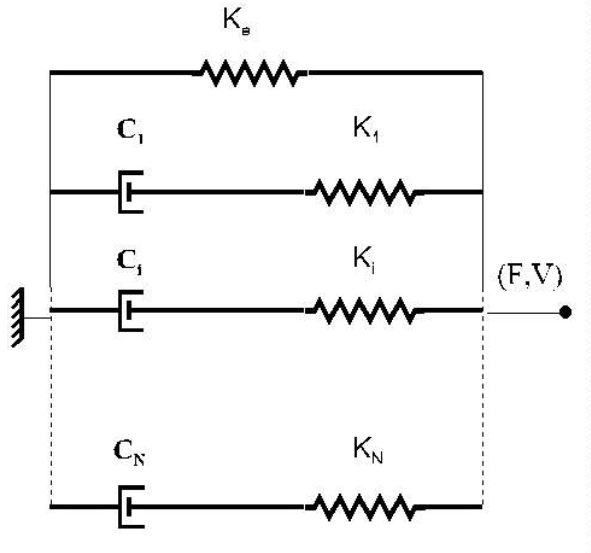

Figure 10: Rheological model equivalent to the finite element model

with:

$$K_e = \frac{2S_0}{l_0}\left(\sum_i \frac{\mu_i}{\alpha_i}\left((\alpha_i - 1)\lambda_0^{\alpha_i - 2} - (-\nu\alpha_i - 1)\lambda_0^{-\nu\alpha_i - 2}\right)\right)\left(1 - \sum_k \varpi_k\right)$$

$$K_i = \frac{2S_0}{l_0}\left(\sum_i \frac{\mu_i}{\alpha_i}\left((\alpha_i - 2)\lambda_0^{\alpha_i - 2} - (-\nu\alpha_i - 2)\lambda_0^{-\nu\alpha_i - 2}\right)\right)\omega_i$$

$$C_i = \frac{2S_0}{l_0}\left(\sum_i \frac{\mu_i}{\alpha_i}\left((\alpha_i - 2)\lambda_0^{\alpha_i - 2} - (-\nu\alpha_i - 2)\lambda_0^{-\nu\alpha_i - 2}\right)\right)\omega_i\tau_i$$

Consequently the rheological model is equivalent to the finite element model, with calculations performed quasi-statically, i.e. masses and inertial forces are not computed. In order to include inertial effects in the model, an element mass was added in parallel to the previous model (see figure 11).

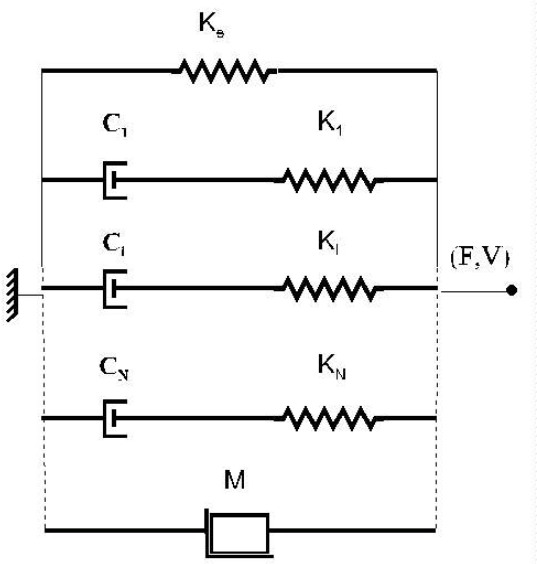

Figure 11: Rheological model including inertial effects

The impedance of the rheological model shown in figure 11 was expressed as [8]:

$$|Z| = \frac{2S_0}{l_0}\left(\sum_i \frac{\mu_i}{\alpha_i}\left((\alpha_i - 2)\lambda_0^{\alpha_i - 2} - (-\nu\alpha_i - 2)\lambda_0^{-\nu\alpha_i - 2}\right)\right)$$

$$\sqrt{\left(\sum_i\left(\frac{\varpi_k\tau_k}{1+\tau_k^{\,2}\omega^2}\right)\right)^2 + \frac{1}{\omega^2}\left(\frac{-\frac{\rho l_0^{\,2}\omega^2}{2} + \left(\sum_i \frac{\mu_i}{\alpha_i}\lambda_0^{\alpha_i - 2} - \lambda_0^{-\nu\alpha_i - 2}\right)\left(1 - \sum_k \varpi_k\right)}{\sum_i \frac{\mu_i}{\alpha_i}\left((\alpha_i - 2)\lambda_0^{\alpha_i - 2} - (-\nu\alpha_i - 2)\lambda_0^{-\nu\alpha_i - 2}\right)} + 1 - \sum_k \frac{\varpi_k}{1+\tau_k^{\,2}\omega^2}\right)^2} \quad \text{eq. 10}$$

where ρ is the material density

The impedance following eq. 10 is reported in figure 12 with following parameters:

- Hyperelastic behavior (given by Wu [4,5]) :

  ν=0.4

  α_1=4.941, α_2=6.425, α_3=4.712

μ_1=-0.07594 MPa, μ_2=0.01138 MPa, μ_3=0.06572 MPa

- Viscous behaviour: (given by Wu [4,5])

τ_1=2.123 s, τ_2=9.371 s

ω_1=0.148, ω_2=0.252

Density:

ρ=1000 kg/m^3

- Model size :

S_0=100 mm², l_0=5 mm

- Initial compression :

λ_0 = 0,5 (correspondant à un effort de pré-compression de 0.4 N)

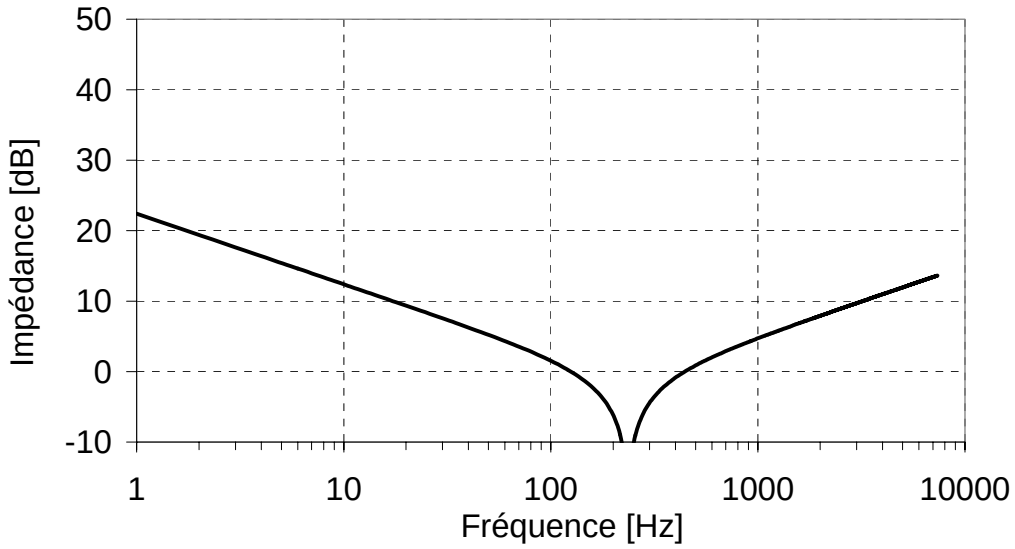

Figure 12 : Impedance of rheological model calculated with the expression 10

The material parameters used to build the figure 12 were taken from Wu [4,5]. Testing parameters were taken as closed as possible from testing parameters given by Lundström in [7]. The resulting calculated impedance has the same shape than the measured impedance reported by Lundström in [7]. Both calculated and measured resonance frequency were found at around 200 Hz.

4. Discussion

Finite Element Method for non linear problems require iterative algorithms to converge to numerical solutions. Commercial softwares embed more or less advanced routines to stabilize calculations but in all cases, no standard method is known to solve automatically non linear problems. In the frame of this work, the materials involved (human tissues) had complex behaviours and the loading conditions (compression + relaxation + vibration) applied to the finger were also complex to deal with. First attempts were made to perform finite element calculations with complex but realistic finger geometries but numerical problems make the model unstable and not sufficient robust to be used. In a second step, only soft tissues localised between the vibrating plate and the phalanx were included in the model The 3D

model, idealized as a parallelepipedic volume, offered the possibility to understand the way used by the Finite Element program to carry out calculations and to express analytically the applied force in response to the rigid plate motion. The following loadcases were applied. First the rigid plate moved at a constant velocity to compress the finger, then was kept still while soft tissues relaxed and finally vibrated at a given frequency. The driving point impedance at the rigid plate during the vibrating phase was calculated and compared to impedance measured by Lündström [7]. Calculated and measured frequency driving point impedances have identical shapes and in both cases a resonance frequency was found at around 200 Hz.

The finite element method is adapted to predict strains and stresses inside a finger exposed to vibration, but the non-linear material behaviour makes calculations difficult to converge. A simpler uniaxial model derived from Finite Element calculations was developed and supplied results like impedances being in agreement with measured impedances reported in the literature. This is encouraging to keep on developing this type of model to have a better understanding of the mechanical response of fingers exposed simultaneously to static force and vibration and therefore to understand reasons for physiological troubles resulting from using vibrating tools.

5. References

[1] John .Z. Wu, Effect of Static Compression on the vibration Modes of a fingertip, Journal of Low frequency Noise, Vibration and Active Control, p. 229-243, Vol. 1 N° 4, 2002

[2] John Z. Wu, Three-dimensional finite element simulations of the mechanical response of the fingertip to static and dynamic compressions, Computer Methods in Biomechanics and Biomedical Engineering, Vol. 9, N° 1, February 2006, 55-63

[3] http://www.eatonhand.com/images/spatch.htm

[4] http://www.code-aster.org

[5] HTML Help-file for the finite element software Samcef version V11.1

[6] Tarek Karoui, Finite Element model to predict vibration behaviour finger (Modélisation du comportement vibratoire d'un doigt par la méthode des éléments finis), Document de travail interne INRS (in French), IET-NP/05DT-118/TK, November 2005

[7] Ronnie Lundström, Local Vibrations – Mechanical Impedance of the Human Hand's Glabrous Skin, J. Biomechanics Vol. 17, N°2, pp. 137-144, 1984

[8] Gérard Fleury, Modélisation du comportement vibratoire d'un volume pré-contraint de chair d'extrémité de doigt, Document de Travail INRS référence IET-NP/07DT/GF, 2007.